International Journal of Engineering Science 53 (2012) 74–84

Contents lists available at SciVerse ScienceDirect

International Journal of Engineering Science

journal homepage: www.elsevier.com/locate/ijengsci

On the asymptotic expansion treatment of two-scale finite thermoelasticity

İ. Temizer *

Department of Mechanical Engineering, Bilkent University, 06800 Ankara, Turkey

ARTICLE INFO

Article history:
Received 19 July 2011
Received in revised form 2 January 2012
Accepted 6 January 2012
Available online 3 February 2012

Keywords:
Finite thermoelasticity
Multiscale
Homogenization
Asymptotic expansion

ABSTRACT

The asymptotic expansion treatment of the homogenization problem for nonlinear purely mechanical or thermal problems exists, together with the treatment of the coupled problem in the linearized setting. In this contribution, an asymptotic expansion approach to homogenization in finite thermoelasticity is presented. The treatment naturally enforces a separation of scales, thereby inducing a first-order homogenization framework that is suitable for computational implementation. Within this framework two microscopically uncoupled cell problems, where a purely mechanical one is followed by a purely thermal one, are obtained. The results are in agreement with a recently proposed approach based on the explicit enforcement of the macroscopic temperature, thereby ensuring thermodynamic consistency across the scales. Numerical investigations additionally demonstrate the computational efficiency of the two-phase homogenization framework in characterizing deformation-induced thermal anisotropy as well as its theoretical advantages in avoiding spurious size effects.

1. Introduction

Homogenization methods provide an efficient framework for addressing the multiscale nature of a large class of boundary value problems. While *higher-order* homogenization frameworks have also been proposed (Forest, Pradel, & Sab, 2001; Kouznetsova, Geers, & Brekelmans, 2004; Larsson & Diebels, 2007), the majority of homogenization approaches are *first-order* in the sense that if $\varepsilon = l_{micro}/l_{macro}$ denotes the ratio between representative length scales associated with the microstructural features and the macrostructural problem then only oscillations of order $\mathcal{O}(\varepsilon^1)$ are taken into account in the resolution of the highly oscillatory fields such as displacement and temperature. In terms of the gradients of these fields, the resolution is of the order $\mathcal{O}(\varepsilon^0)$, which corresponds to the classical separation of scales assumption $l_{micro} \ll l_{macro}$, or $\varepsilon \to 0$. A formal resolution of the oscillatory solution fields is based on the *asymptotic expansion* (AE) approach that goes back to the work of Sanchez-Palencia (1980). See also Torquato (2002) and Pavliotis and Stuart (2008) for recent overviews. The goal of this contribution is to highlight the AE basis for a homogenization framework in finite thermoelasticity that was recently proposed in Temizer and Wriggers (2011). A concise presentation is pursued with references exclusively concentrating on works where an explicit AE approach has been investigated for thermomechanical problems. See Temizer and Wriggers (2011) for extensive references on closely related approaches in various multiphysics problems.

The background on homogenization in finite thermoelasticity has three major branches. The first takes into account the finite deformation kinematics in purely mechanical problems. While an AE treatment in the infinitesimal deformation regime is well-known (Sanchez-Palencia, 1980), extensions to large deformations were first discussed in Takano, Ohnishi, Zako, and Nishiyabu (2000) and subsequently developed in detail by Terada, Saiki, Matsui, and Yamakawa (2003) where the algorithmic tangents associated with the Newton–Raphson type iterative solution of the nonlinear macroscopic

* Tel.: +90 (312) 290 3064.
E-mail address: temizer@bilkent.edu.tr

0020-7225/$ - see front matter © 2012 Elsevier Ltd. All rights reserved.
doi:10.1016/j.ijengsci.2012.01.003

boundary value problem were additionally derived. See also Fish and Fan (2008). As the second branch of concern, an AE treatment of nonlinear thermal conduction in a rigid heterogeneous medium was addressed first in Laschet (2002) in a quasistatic setting while the treatment of the linearized setting is again well-known (Sanchez-Palencia, 1980). As the final branch, the first treatment of the coupled transient thermoelasticity problem in a linearized setting was presented in Francfort (1983). The coupled quasistatic problem was further investigated by Alzina, Toussaint, and Béakou (2007) while the transient case with viscous dissipation effects was considered in Francfort (1986) and Yu and Fish (2002) and recently with fluid-filled porous materials in Terada, Kurumatani, Ushida, and Kikuchi (2010). To the best knowledge of the author, an AE approach for the coupled thermoelasticity problem with finite deformation kinematics, nonlinear thermal conduction and large deviations from the equilibrium temperature has not been presented in the literature.

Computational approaches for the coupled nonlinear thermomechanical problem that are motivated by single-physics homogenization techniques have been presented in a limited number of works, among them Miehe, Schröder, and Schotte (1999), Aboudi (2002), Khisaeva and Ostoja-Starzewski (2007) and Özdemir, Brekelmans, and Geers (2008). These approaches were critically examined in Temizer and Wriggers (2011) and two major shortcomings were pointed out in the literature: (i) the coupled nature of the macroscopic boundary value problem has not been investigated to full extent in a transient setting, and (ii) a separation of scales assumption has not been preserved. While the first shortcoming is important from a numerical point of view, the second one is essential in order to avoid non-physical size effects and confirm consistency with earlier single-physics approaches. With a view towards addressing these shortcomings, a framework was presented in Temizer and Wriggers (2011) based on the explicit constitutive formulation in finite thermoelasticity (Chadwick & Creasy, 1984). It was demonstrated that in order to preserve thermodynamic consistency across the scale transitions, i.e. to obtain the classical finite thermoelasticity formulation on the macroscale as well, the homogenization approach must be based on an explicit enforcement of the macroscopic temperature which naturally induces a two-phase computational framework. Within this framework, (i) a purely mechanical microstructural problem is solved on a test sample by imposing the macroscopic deformation gradient as boundary conditions while the temperature is uniformly elevated to its macroscopic counterpart throughout the whole sample, followed by (ii) a purely thermal one where a nonlinear thermal conduction problem is solved on the frozen configuration from the first phase. The first phase delivers the macroscopic stress while the second delivers the macroscopic heat flux.

While the mentioned two-phase computational setup closely resembles the classical numerical staggering schemes (Simo, 1998), it was emphasized in Temizer and Wriggers (2011) that this framework is not a numerical approximation but rather it is exact to within a separation of scales assumption. In this contribution, the separation of scales is explicitly invoked within an AE treatment and it is demonstrated that the mentioned two-phase computational homogenization framework is recovered. For this purpose, the balance laws governing finite thermoelasticity are briefly summarized in Section 2. The AEs of the thermomechanical primal and dual variables are introduced in Section 3 where various homogenization results are also recalled. Finally, the cell problems of homogenization are obtained in Section 4 together with the macroscopic transient boundary value problems. Practical implications of the obtained results are discussed in detail. While the emphasis is strictly on the AE treatment, novel numerical results are presented that complement the investigations of Temizer and Wriggers (2011) in the context of deformation-induced thermal anisotropy and spurious size effects. See also Temizer and Wriggers (2011) for extensive numerical investigations together with additional discussions on the macroscopic thermodynamics and numerics.

2. Finite thermoelasticity

Let $\boldsymbol{X}$ and $\boldsymbol{x}$ denote the position vectors with respect to the reference ($\mathcal{R}$) and current configurations of a body $\mathcal{B}$ such that $\boldsymbol{u} = \boldsymbol{x} - \boldsymbol{X}$ corresponds to the displacement field while $\boldsymbol{N}$ denotes the outward unit normal to $\mathcal{R}$. For the purposes of this work, the reference configuration of a body coincides with the undeformed configuration at a uniform reference temperature θ_{REF} while the current configuration is assigned a distribution $\theta(\boldsymbol{X})$. Exclusively pursuing a finite thermoelasticity formulation, Grad[•] and Div[•] indicate the associated gradient and divergence operators with respect to the reference configuration. Consequently, $\boldsymbol{F} = \text{Grad}[\boldsymbol{x}]$ and $\boldsymbol{G} = \text{Grad}[\theta]$ indicate the (deformation and temperature) gradient fields using which the general constitutive forms $\boldsymbol{P}(\theta,\boldsymbol{F})$ for the 1st Piola–Kirchhoff stress tensor and $\boldsymbol{Q}(\theta,\boldsymbol{G},\boldsymbol{F})$ for the heat flux vector are admitted. $\{\boldsymbol{x},\boldsymbol{u},\theta\}$ will be referred to as *primal* quantities while *dual* will be employed to refer to $\{\boldsymbol{P},\boldsymbol{Q}\}$. Explicit constitutive formulations are presently not required.

Admitting a standard continuum, the angular momentum balance is assumed to be satisfied *a priori* : $\boldsymbol{P}\boldsymbol{F}^T = \boldsymbol{F}\boldsymbol{P}^T$. The linear momentum balance requires (ρ : density in $\mathcal{R}$)

$$\text{Div}[\boldsymbol{P}] + \boldsymbol{f} = \rho\ddot{\boldsymbol{u}} \tag{2.1}$$

in $\mathcal{R}$, with $\boldsymbol{f}$ as a body force per unit volume of $\mathcal{R}$, subject to the specification of $\boldsymbol{x}$ or $\boldsymbol{p} = \boldsymbol{P}\boldsymbol{N}$ on a suitable partitioning of the boundary $\partial\mathcal{R}$. In a similar fashion, using c to denote the specific heat at constant deformation per unit volume of $\mathcal{R}$, the energy balance for finite thermoelasticity can be expressed in the reduced form

$$c\dot{\theta} = \theta\frac{\partial \boldsymbol{P}}{\partial\theta}\cdot\dot{\boldsymbol{F}} - \text{Div}[\boldsymbol{Q}] + r, \tag{2.2}$$

with appropriate boundary conditions on θ or $h = -\boldsymbol{Q}\cdot\boldsymbol{N}$. The first term on the right-hand side is responsible for the Gough-Joule effect and r is a heat supply per unit volume of $\mathcal{R}$. For future reference, the stress power is denoted by $\mathcal{P} = \boldsymbol{P}\cdot\dot{\boldsymbol{F}}$.

Herein, the existence of a Helmholtz free energy function $\Psi(\theta,\boldsymbol{F})$ (per unit volume of $\mathcal{R}$) has been admitted such that $c = -\theta(\partial^2\Psi/\partial\theta^2)$ and the second law of thermodynamics condenses to the requirements (Maugin, 1999)

$$\boldsymbol{P} = \frac{\partial\Psi}{\partial\boldsymbol{F}}, \quad \mathcal{D} = -\frac{\boldsymbol{Q}\cdot\boldsymbol{G}}{\theta} \geqslant 0. \tag{2.3}$$

The latter expression is the statement of a positive dissipation, which is purely thermal due to the absence of any mechanical dissipation within a thermoelastic setting, and is assumed to be satisfied by the form of $\boldsymbol{Q}$. A general expression for the functional form of Ψ may easily be constructed (Chadwick & Creasy, 1984) – see also Temizer and Wriggers (2011) and Section 5.

3. Two-scale representation

3.1. Asymptotic expansion

The body $\mathcal{B}$ is admitted to be materially inhomogeneous at a fine scale (or, *microheterogeneous*). Following a classical mathematical construction (Pavliotis & Stuart, 2008; Sanchez-Palencia, 1980; Torquato, 2002), the nature of the heterogeneities is assigned a two-scale *periodic* structure that is represented by a macroscale (referential) position vector $\boldsymbol{X}$ and its microscale counterpart $\boldsymbol{Y} = \boldsymbol{X}/\varepsilon$ such that $\varepsilon \to 0$, i.e. *scale separation is enforced*. In the context of AE, $\{\boldsymbol{X},\boldsymbol{Y}\}$ are subsequently treated as independent variables. The *unit cell* characterizing local periodicity at a macroscale position $\boldsymbol{X}$ is denoted $\mathcal{Y}$. The highly-oscillatory primal variables $\boldsymbol{u}_\varepsilon$ and θ_ε are then assumed to have the AEs

$$\boldsymbol{u}_\varepsilon(\boldsymbol{X}) = \boldsymbol{u}(\boldsymbol{X},\boldsymbol{Y}) = \boldsymbol{u}_o(\boldsymbol{X},\boldsymbol{Y}) + \varepsilon\boldsymbol{u}_1(\boldsymbol{X},\boldsymbol{Y}) + \varepsilon^2\boldsymbol{u}_2(\boldsymbol{X},\boldsymbol{Y}) + \mathcal{O}(\varepsilon^3) \tag{3.1}$$

and

$$\theta_\varepsilon(\boldsymbol{X}) = \theta(\boldsymbol{X},\boldsymbol{Y}) = \theta_o(\boldsymbol{X},\boldsymbol{Y}) + \varepsilon\theta_1(\boldsymbol{X},\boldsymbol{Y}) + \varepsilon^2\theta_2(\boldsymbol{X},\boldsymbol{Y}) + \mathcal{O}(\varepsilon^3). \tag{3.2}$$

Here and in the following developments, the notation

$$[\bullet]_o := \lim_{\varepsilon\to 0}[\bullet] \tag{3.3}$$

will be consistently employed. It is assumed that the heterogeneous continuum is initially in mechanical and thermal equilibrium. The latter requires, in particular, that $\theta = \theta_o = \theta_{REF}$ initially. In addition to the $\mathcal{Y}$-periodicity of the microstructure, $\boldsymbol{u}_i$ and θ_i are also assigned a $\mathcal{Y}$-periodic structure. Moreover, it is assumed that there are no discontinuities in these fields. As $\varepsilon \to 0$, only the explicit solution of the *first-order corrector* (or, *fluctuation*) fields $\{\boldsymbol{u}_1,\theta_1\}$ are of interest.

The differential operators can be expanded in partial derivatives as

$$\mathrm{Div}[\bullet] = \mathrm{Div}_{\boldsymbol{X}}[\bullet] + \frac{1}{\varepsilon}\mathrm{Div}_{\boldsymbol{Y}}[\bullet], \quad \mathrm{Grad}[\bullet] = \mathrm{Grad}_{\boldsymbol{X}}[\bullet] + \frac{1}{\varepsilon}\mathrm{Grad}_{\boldsymbol{Y}}[\bullet]. \tag{3.4}$$

Consequently, using $\boldsymbol{I}$ to denote the identity tensor, the induced gradient fields have the expansions

$$\boldsymbol{F} = \frac{1}{\varepsilon}\mathrm{Grad}_{\boldsymbol{Y}}[\boldsymbol{u}_o] + \underbrace{\boldsymbol{I} + \mathrm{Grad}_{\boldsymbol{X}}[\boldsymbol{u}_o] + \mathrm{Grad}_{\boldsymbol{Y}}[\boldsymbol{u}_1]}_{=:\boldsymbol{F}_o} + \varepsilon(\mathrm{Grad}_{\boldsymbol{X}}[\boldsymbol{u}_1] + \mathrm{Grad}_{\boldsymbol{Y}}[\boldsymbol{u}_2]) + \mathcal{O}(\varepsilon^2) \tag{3.5}$$

and

$$\boldsymbol{G} = \frac{1}{\varepsilon}\mathrm{Grad}_{\boldsymbol{Y}}[\theta_o] + \underbrace{\mathrm{Grad}_{\boldsymbol{X}}[\theta_o] + \mathrm{Grad}_{\boldsymbol{Y}}[\theta_1]}_{=:\boldsymbol{G}_o} + \varepsilon(\mathrm{Grad}_{\boldsymbol{X}}[\theta_1] + \mathrm{Grad}_{\boldsymbol{Y}}[\theta_2]) + \mathcal{O}(\varepsilon^2). \tag{3.6}$$

Now, if $\boldsymbol{F}$ and $\boldsymbol{G}$ are to remain bounded in the limit as $\varepsilon \to 0$, it is required that

$$\mathrm{Grad}_{\boldsymbol{Y}}[\boldsymbol{u}_o] = \boldsymbol{0}, \quad \mathrm{Grad}_{\boldsymbol{Y}}[\theta_o] = \boldsymbol{0}, \tag{3.7}$$

which is simply a statement that $\boldsymbol{u}_o$ and θ_o are independent of $\boldsymbol{Y}$. In the classical linearized framework for single-and multiphysics settings, this result is automatically induced through an explicit expansion of the balance laws (Pavliotis & Stuart, 2008; Sanchez-Palencia, 1980; Terada et al., 2010; Yu & Fish, 2002). Making use of these expansions together with the *cell average*

$$\langle\bullet\rangle = \frac{1}{|\mathcal{Y}|}\int_{\mathcal{Y}} \bullet \, \mathrm{d}\mathcal{Y} \tag{3.8}$$

it is straightforward to verify the standard relationships between macroscopic and microscopic quantities:

$$\overline{\boldsymbol{F}} := \boldsymbol{I} + \mathrm{Grad}_{\boldsymbol{X}}[\boldsymbol{u}_o] = \langle\boldsymbol{F}_o\rangle, \quad \overline{\boldsymbol{G}} := \mathrm{Grad}_{\boldsymbol{X}}[\theta_o] = \langle\boldsymbol{G}_o\rangle. \tag{3.9}$$

The macroscopic temperature is already represented by θ_o and it does *not* correspond to a cell average. To summarize, the local deformation and temperature distributions are controlled by $\{\theta_o(\boldsymbol{X}), \overline{\boldsymbol{G}}(\boldsymbol{X}), \overline{\boldsymbol{F}}(\boldsymbol{X})\}$ only.

3.2. Expansion of the dual variables

Finally, in order to construct an expansion of the dual variables without specifying the particular constitutive choices, the microscale mechanical sensitivities

$$\boldsymbol{M} = \frac{\partial \boldsymbol{P}}{\partial \theta}, \qquad \boldsymbol{IK} = \frac{\partial \boldsymbol{P}}{\partial \boldsymbol{F}} \tag{3.10}$$

and their thermal counterparts

$$\boldsymbol{m} = \frac{\partial \boldsymbol{Q}}{\partial \theta}, \qquad \boldsymbol{K} = \frac{\partial \boldsymbol{Q}}{\partial \boldsymbol{G}} \quad , \quad \boldsymbol{\mathcal{Q}} = \frac{\partial \boldsymbol{Q}}{\partial \boldsymbol{F}} \tag{3.11}$$

are introduced. While the sensitivity of $\boldsymbol{Q}$ with respect to $\boldsymbol{G}$ classically involves a negative sign, the present choice is made for simplicity. One may then proceed to the expansion of the stress via

$$\begin{aligned}\boldsymbol{P}(\theta,\boldsymbol{F}) &= \boldsymbol{P}(\theta,\boldsymbol{F})|_{\varepsilon=0} + \varepsilon \left.\frac{\mathrm{d}\boldsymbol{P}}{\mathrm{d}\varepsilon}\right|_{\varepsilon=0} + \mathcal{O}(\varepsilon^2) = \boldsymbol{P}_o + \varepsilon\left(\boldsymbol{M}\frac{\partial\theta}{\partial\varepsilon} + \boldsymbol{IK}\frac{\partial \boldsymbol{F}}{\partial\varepsilon}\right)\Big|_{\varepsilon=0} + \mathcal{O}(\varepsilon^2)\\ &= \boldsymbol{P}_o + \varepsilon(\boldsymbol{M}_o\theta_1 + \boldsymbol{IK}_o\{\mathrm{Grad}_{\boldsymbol{X}}[\boldsymbol{u}_1] + \mathrm{Grad}_{\boldsymbol{Y}}[\boldsymbol{u}_2]\}) + \mathcal{O}(\varepsilon^2),\end{aligned} \tag{3.12}$$

where $\boldsymbol{P}_o := \boldsymbol{P}(\theta_o, \boldsymbol{F}_o)$. In a similar fashion, the expansion of the heat flux vector is found to be

$$\boldsymbol{Q}(\theta,\boldsymbol{G},\boldsymbol{F}) = \boldsymbol{Q}_o + \varepsilon(\boldsymbol{m}_o\theta_1 + \boldsymbol{K}_o\{\mathrm{Grad}_{\boldsymbol{X}}[\theta_1] + \mathrm{Grad}_{\boldsymbol{Y}}[\theta_2]\} + \boldsymbol{\mathcal{Q}}_o\{\mathrm{Grad}_{\boldsymbol{X}}[\boldsymbol{u}_1] + \mathrm{Grad}_{\boldsymbol{Y}}[\boldsymbol{u}_2]\}) + \mathcal{O}(\varepsilon^2), \tag{3.13}$$

where $\boldsymbol{Q}_o := \boldsymbol{Q}(\theta_o, \boldsymbol{G}_o, \boldsymbol{F}_o)$. Due to the assumed $\mathcal{Y}$-periodicity, $\boldsymbol{p}$ and h are anti-periodic on $\partial\mathcal{Y}$.

It is also useful to expand the body force and heat supply terms. Based on the relatively general forms $\boldsymbol{f}(\theta,\boldsymbol{u})$ and $r(\theta,\boldsymbol{u})$, the expansions

$$\boldsymbol{f}(\theta,\boldsymbol{u}) = \boldsymbol{f}_o + \mathcal{O}(\varepsilon), \quad r(\theta,\boldsymbol{u}) = r_o + \mathcal{O}(\varepsilon) \tag{3.14}$$

hold with respect to $\boldsymbol{u}$ and θ, respectively, where $\boldsymbol{f}_o := \boldsymbol{f}(\theta_o, \boldsymbol{u}_o)$ and $r_o := r(\theta_o, \boldsymbol{u}_o)$. Clearly, a similar expansion follows for all quantities that depend on any of the fields $\{\theta, \boldsymbol{u}, \boldsymbol{F}\}$, in particular for $\{\Psi, c, \mathcal{P}, \mathcal{D}\}$:

$$\Psi_o = \Psi(\theta_o, \boldsymbol{F}_o), \quad c_o = -\theta_o\frac{\partial^2\Psi_o}{\partial\theta_o^2}, \quad \mathcal{P}_o = \boldsymbol{P}_o\cdot\dot{\boldsymbol{F}}_o, \quad \mathcal{D}_o = -\frac{\boldsymbol{Q}_o\cdot\boldsymbol{G}_o}{\theta_o}. \tag{3.15}$$

It is noted that, while not explicitly denoted, all of these quantities have a dependence on $\{\boldsymbol{X}, \boldsymbol{Y}\}$.

4. Two-scale boundary value problem

4.1. Linear momentum balance

The substitution of (3.12) into (2.1), making use of (3.4) and explicitly retaining only terms of order ε^0 or less leads to:

$$\begin{aligned}\rho\ddot{\boldsymbol{u}}_o + \mathcal{O}(\varepsilon) &= \left(\mathrm{Div}_{\boldsymbol{X}}[\boldsymbol{P}] + \frac{1}{\varepsilon}\mathrm{Div}_{\boldsymbol{Y}}[\boldsymbol{P}]\right) + \boldsymbol{f}_o + \mathcal{O}(\varepsilon)\\ &= \mathrm{Div}_{\boldsymbol{X}}[\boldsymbol{P}_o] + \mathrm{Div}_{\boldsymbol{Y}}[\boldsymbol{M}_o\theta_1 + \boldsymbol{IK}_o\{\mathrm{Grad}_{\boldsymbol{X}}[\boldsymbol{u}_1] + \mathrm{Grad}_{\boldsymbol{Y}}[\boldsymbol{u}_2]\}] + \boldsymbol{f}_o + \frac{1}{\varepsilon}\mathrm{Div}_{\boldsymbol{Y}}[\boldsymbol{P}_o] + \mathcal{O}(\varepsilon).\end{aligned} \tag{4.1}$$

Note that ρ does not have an AE with respect to any of the fields $\{\theta, \boldsymbol{u}, \boldsymbol{F}\}$ and therefore is retained in its original form.

In the limit as $\varepsilon \to 0$, this expansion implies two results. First, $\mathcal{O}(\varepsilon^{-1})$ term induces

$$\mathrm{Div}_{\boldsymbol{Y}}[\boldsymbol{P}_o] = \boldsymbol{0} \tag{4.2}$$

or, explicitly denoting $\boldsymbol{P}_o$,

$$\boxed{\mathrm{Div}_{\boldsymbol{Y}}[\boldsymbol{P}(\theta_o, \boldsymbol{F}_o)] = \boldsymbol{0}.} \tag{4.3}$$

This is a classical cell problem in $\mathcal{Y}$. Its significance lies in the fact that *only the macroscopic temperature θ_o enters the cell problem explicitly*. In other words, the temperature distribution that is locally induced by the temperature gradient $\boldsymbol{G}_o$ does not influence the stress distribution within $\mathcal{Y}$ under the separation of scales assumption $\varepsilon \to 0$. Consequently, a *purely mechanical cell problem* is obtained which is solved at an elevated (or, reduced) temperature θ_o that is uniform throughout the cell. Since $\boldsymbol{P}_o$ is nonlinear in $\boldsymbol{F}_o$, this cell problem is solved iteratively for the $\boldsymbol{u}_1$ term, that is unique to within a rigid body translation, while enforcing $\langle \boldsymbol{F}_o \rangle = \overline{\boldsymbol{F}}$.

As the second result of the expansion (4.1), terms of order ε^0 imply, after rearranging,

$$\mathrm{Div}_{\boldsymbol{Y}}[\boldsymbol{I}\boldsymbol{K}_o\mathrm{Grad}_{\boldsymbol{Y}}[\boldsymbol{u}_2]] = \rho\ddot{\boldsymbol{u}}_o - \boldsymbol{f}_o - \mathrm{Div}_{\boldsymbol{X}}[\boldsymbol{P}_o] - \mathrm{Div}_{\boldsymbol{Y}}[\boldsymbol{M}_o\theta_1 + \boldsymbol{I}\boldsymbol{K}_o\mathrm{Grad}_{\boldsymbol{X}}[\boldsymbol{u}_1]]. \tag{4.4}$$

Here, the classical condition is invoked, namely that for this equation to have a $\mathcal{Y}$-periodic solution $\boldsymbol{u}_2$ the cell average of the right-hand side must vanish (Pavliotis & Stuart, 2008):

$$\langle \mathrm{Div}_{\boldsymbol{X}}[\boldsymbol{P}_o] + \mathrm{Div}_{\boldsymbol{Y}}[\boldsymbol{M}_o\theta_1 + \boldsymbol{I}\boldsymbol{K}_o\mathrm{Grad}_{\boldsymbol{X}}[\boldsymbol{u}_1]] + \boldsymbol{f}_o - \rho\ddot{\boldsymbol{u}}_o\rangle = \boldsymbol{0}. \tag{4.5}$$

It is remarked that, since $\boldsymbol{X}$ and $\boldsymbol{Y}$ are treated as independent variables, $\boldsymbol{X}$ enters all functional dependencies only as a parameter such that $\langle\bullet\rangle$ is interchangeable with $\mathrm{Grad}_{\boldsymbol{X}}[\bullet]$ and $\mathrm{Div}_{\boldsymbol{X}}[\bullet]$. The terms within $\mathrm{Div}_{\boldsymbol{Y}}[\bullet]$ vanish after cell-averaging due to their periodicity, upon making use of the divergence theorem. Consequently, the induced equation corresponds to the *macroscopic linear momentum balance* and reads

$$\boxed{\mathrm{Div}_{\boldsymbol{X}}[\langle\boldsymbol{P}_o\rangle] + \langle\boldsymbol{f}_o\rangle = \langle\rho\rangle\ddot{\boldsymbol{u}}_o,} \tag{4.6}$$

where $\langle\boldsymbol{P}_o\rangle =: \overline{\boldsymbol{P}}$ corresponds to the *macroscopic stress*, $\langle\boldsymbol{f}_o\rangle =: \bar{\boldsymbol{f}}$ is the *macroscopic body force* term and $\langle\rho\rangle =: \bar{\rho}$ is the *macroscopic density*. Clearly, $\overline{\boldsymbol{P}}$ is governed by the microstructure and $\{\theta_o, \overline{\boldsymbol{F}}\}$, and hence depends implicitly on $\boldsymbol{X}$, but does not depend on $\boldsymbol{Y}$ due to cell-averaging. All results are in close similarity with the purely mechanical case (Terada et al., 2003).

The divergence-free nature of $\boldsymbol{P}_o$ together with the periodicity conditions ensure the classical transition

$$\langle\mathcal{P}_o\rangle = \langle\boldsymbol{P}_o\cdot\dot{\boldsymbol{F}}_o\rangle = \langle\boldsymbol{P}_o\rangle\cdot\langle\dot{\boldsymbol{F}}_o\rangle = \overline{\boldsymbol{P}}\cdot\dot{\overline{\boldsymbol{F}}} =: \overline{\mathcal{P}}, \tag{4.7}$$

where $\overline{\mathcal{P}}$ is the *macroscopic stress power*, which is referred to as the *micro–macro work equality* (or, *Hill–Mandel macrohomogeneity condition*) in the engineering literature. This condition can alternatively be regarded as the starting point for designing boundary conditions which are not periodic within practical homogenization setups – see Temizer and Wriggers (2011) for extensive references.

4.2. Energy balance

Similar to Section 4.1, the substitution of (3.13) into (2.2), making use of (3.4) and explicitly retaining only terms of order ε^0 or less leads to:

$$\begin{aligned} c_o\,\dot{\theta}_o + \mathcal{O}(\varepsilon) = \theta_o\boldsymbol{M}_o\cdot\dot{\boldsymbol{F}}_o - \left(\mathrm{Div}_{\boldsymbol{X}}[\boldsymbol{Q}] + \frac{1}{\varepsilon}\mathrm{Div}_{\boldsymbol{Y}}[\boldsymbol{Q}]\right) + r_o + \mathcal{O}(\varepsilon) = \theta_o\boldsymbol{M}_o\cdot\dot{\boldsymbol{F}}_o - \mathrm{Div}_{\boldsymbol{X}}[\boldsymbol{Q}_o] \\ - \mathrm{Div}_{\boldsymbol{Y}}[\boldsymbol{m}_o\theta_1 + \boldsymbol{K}_o\{\mathrm{Grad}_{\boldsymbol{X}}[\theta_1] + \mathrm{Grad}_{\boldsymbol{Y}}[\theta_2]\} + \mathcal{Q}_o\{\mathrm{Grad}_{\boldsymbol{X}}[\boldsymbol{u}_1] + \mathrm{Grad}_{\boldsymbol{Y}}[\boldsymbol{u}_2]\}] - \frac{1}{\varepsilon}\mathrm{Div}_{\boldsymbol{Y}}[\boldsymbol{Q}_o] + r_o + \mathcal{O}(\varepsilon). \end{aligned} \tag{4.8}$$

In the limit as $\varepsilon\to 0$, this expansion also implies two results. First, $\mathcal{O}(\varepsilon^{-1})$ term induces the cell problem

$$-\mathrm{Div}_{\boldsymbol{Y}}[\boldsymbol{Q}_o] = \boldsymbol{0}, \tag{4.9}$$

or, explicitly denoting $\boldsymbol{Q}_o$,

$$\boxed{-\mathrm{Div}_{\boldsymbol{Y}}[\boldsymbol{Q}(\theta_o, \boldsymbol{G}_o, \boldsymbol{F}_o)] = \boldsymbol{0}.} \tag{4.10}$$

Its significance is twofold. First, only the macroscopic temperature θ_o enters the cell problem and hence the temperature distribution induced by $\boldsymbol{G}_o$ does not influence temperature-dependent thermal material properties. These are evaluated at the elevated macroscopic temperature θ_o. Second, $\boldsymbol{F}_o$ is transferred from the solution to the purely mechanical cell problem (4.3). In other words, (4.10) is a *purely thermal cell problem* that is solved at the frozen (deformed) configuration that is inherited from the mechanical one. Since $\boldsymbol{Q}_o$ is possibly nonlinear in $\boldsymbol{G}_o$, this cell problem is solved iteratively for the θ_1 term, that is unique to within a constant shift of the temperature, while enforcing $\langle\boldsymbol{G}_o\rangle = \overline{\boldsymbol{G}}$.

It is important to highlight that, as delineated in Temizer and Wriggers (2011), the uncoupling among the mechanical and thermal problems on the microscale cell problem is *not* a numerical (e.g. operator-split type) approximation. Rather, it is an exact theoretical split that is a consequence of the separation of scales assumption $\varepsilon\to 0$.

As the second result of the expansion (4.8), terms of order ε^0 imply

$$\mathrm{Div}_{\boldsymbol{Y}}[\boldsymbol{K}_o\mathrm{Grad}_{\boldsymbol{Y}}[\theta_2]] = -c_o\dot{\theta}_o + \theta_o\boldsymbol{M}_o\cdot\dot{\boldsymbol{F}}_o - \mathrm{Div}_{\boldsymbol{X}}[\boldsymbol{Q}_o] + r_o - \mathrm{Div}_{\boldsymbol{Y}}[\boldsymbol{m}_o\theta_1 + \boldsymbol{K}_o\mathrm{Grad}_{\boldsymbol{X}}[\theta_1] + \mathcal{Q}_o\{\mathrm{Grad}_{\boldsymbol{X}}[\boldsymbol{u}_1] + \mathrm{Grad}_{\boldsymbol{Y}}[\boldsymbol{u}_2]\}]. \tag{4.11}$$

Here, the mechanical terms have been retained on the right-hand side together with all the other variables which can be numerically evaluated. Consequently, the existence of a $\mathcal{Y}$-periodic solution to the unknown term θ_2 requires that the cell average of the right-hand side vanishes (Pavliotis & Stuart, 2008). Using the periodicity of all terms within $\mathrm{Div}_{\boldsymbol{Y}}[\cdot]$, the requirement reads

$$\boxed{\langle c_o\rangle\,\dot{\theta}_o = \theta_o\langle\boldsymbol{M}_o\cdot\dot{\boldsymbol{F}}_o\rangle - \mathrm{Div}_{\boldsymbol{X}}[\langle\boldsymbol{Q}_o\rangle] + \langle r_o\rangle} \tag{4.12}$$

where $\langle \boldsymbol{Q}_o \rangle =: \overline{\boldsymbol{Q}}$ corresponds to the *macroscopic heat flux* and $\langle r_o \rangle =: \bar{r}$ is the *macroscopic heat supply* term. This is the finite thermoelasticity counterpart of the result in Yu and Fish (2002). Similar to the linear momentum balance, $\overline{\boldsymbol{Q}}$ is governed by the microstructure and $\{\theta_o, \overline{\boldsymbol{G}}, \overline{\boldsymbol{F}}\}$, and hence depends implicitly on $\boldsymbol{X}$, but does not depend on $\boldsymbol{Y}$ due to cell-averaging.

As for its mechanical counterpart (4.7), the divergence-free nature of $\boldsymbol{Q}_o$ together with the periodicity conditions ensure the transition

$$\langle \mathcal{D}_o \rangle = \left\langle -\frac{\boldsymbol{Q}_o \cdot \boldsymbol{G}_o}{\theta_o} \right\rangle = -\frac{\langle \boldsymbol{Q}_o \rangle \cdot \langle \boldsymbol{G}_o \rangle}{\theta_o} = -\frac{\overline{\boldsymbol{Q}} \cdot \overline{\boldsymbol{G}}}{\theta_o} =: \overline{\mathcal{D}}, \tag{4.13}$$

where $\overline{\mathcal{D}}$ is the *macroscopic thermal dissipation*, which is a micro–macro (thermal) dissipation equality. The identities (4.7) and (4.13) together ensure that the microscale mechanical work and thermal dissipation are preserved through the scale transition.

While (4.12) represents the *macroscopic energy balance*, it is not of the form (2.2) that is expected for the macroscopic thermoelastic medium, i.e. the macroscopic quantities are expected to satisfy

$$\boxed{\bar{c}\dot{\theta}_o = \theta_o \tfrac{\partial \overline{\boldsymbol{P}}}{\partial \theta_o} \cdot \dot{\overline{\boldsymbol{F}}} - \mathrm{Div}_{\boldsymbol{X}}[\overline{\boldsymbol{Q}}] + \bar{r}.} \tag{4.14}$$

In order to restate (4.12) in this convenient form, the *macroscopic specific heat* $\bar{c}$ is characterized in the next section. It is remarked that the form (4.14) is strictly an expectation on the basis of a separation of scales. Otherwise, a macroscopically viscous response may be observed (Molinari & Ortiz, 1987). For heterogeneities that are small but not too small, the extent to which the assumption of a purely thermoelastic macroscopic response is suitable also depends on the relevant time scales of the problem (Molinari & Ortiz, 1987; Yu & Fish, 2002).

4.3. Macroscopic specific heat

Since $\boldsymbol{P}_o = \boldsymbol{P}(\theta_o, \boldsymbol{F}_o)$, one can reexpress $\boldsymbol{M}_o$ as

$$\boldsymbol{M}_o = \left.\frac{\partial \boldsymbol{P}}{\partial \theta}\right|_{\varepsilon=0} = \frac{\partial \boldsymbol{P}_o}{\partial \theta_o} = \frac{\mathrm{d}\boldsymbol{P}_o}{\mathrm{d}\theta_o} - \frac{\partial \boldsymbol{P}_o}{\partial \boldsymbol{F}_o}\frac{\partial \boldsymbol{F}_o}{\partial \theta_o}, \tag{4.15}$$

where use has been made of the fact that the $\boldsymbol{F}_o$ distribution, but not its cell average $\langle \boldsymbol{F}_o \rangle = \overline{\boldsymbol{F}}$, depends on the macroscopic temperature θ_o. Consequently, the cell-averaged Gough–Joule term may be expanded as

$$\theta_o \langle \boldsymbol{M}_o \cdot \dot{\boldsymbol{F}}_o \rangle = \theta_o \left\langle \frac{\mathrm{d}\boldsymbol{P}_o}{\mathrm{d}\theta_o} \cdot \dot{\boldsymbol{F}}_o \right\rangle - \theta_o \left\langle \frac{\partial \boldsymbol{P}_o}{\partial \boldsymbol{F}_o}\frac{\partial \boldsymbol{F}_o}{\partial \theta_o} \cdot \dot{\boldsymbol{F}}_o \right\rangle, \tag{4.16}$$

where the first term on the right-hand side can be further simplified to

$$\theta_o \left\langle \frac{\mathrm{d}\boldsymbol{P}_o}{\mathrm{d}\theta_o} \cdot \dot{\boldsymbol{F}}_o \right\rangle = \theta_o \frac{\partial \langle \boldsymbol{P}_o \rangle}{\partial \theta_o} \cdot \langle \dot{\boldsymbol{F}}_o \rangle = \theta_o \frac{\partial \overline{\boldsymbol{P}}}{\partial \theta_o} \cdot \dot{\overline{\boldsymbol{F}}}, \tag{4.17}$$

which is exactly the macroscopic Gough–Joule term. Here, the transition to the second equality is performed, as in the transition (4.7), by making use of the periodic boundary conditions and the divergence-free nature of $\frac{\mathrm{d}\boldsymbol{P}_o}{\mathrm{d}\theta_o}$, the latter stating that $\boldsymbol{P}_o$ satisfies the cell problem (4.3) for all choices of θ_o at a fixed macroscopic deformation $\overline{\boldsymbol{F}}$. Note that $\frac{\partial \boldsymbol{P}_o}{\partial \theta_o}$ alone is not divergence-free since a constant $\boldsymbol{F}_o$ distribution while θ_o is varied does not satisfy local equilibrium.

Combining (4.16) and (4.17), the macroscopic energy balance (4.12) may be restated in the convenient form

$$\langle c_o \rangle \dot{\theta}_o + \theta_o \left\langle \frac{\partial \boldsymbol{P}_o}{\partial \boldsymbol{F}_o}\frac{\partial \boldsymbol{F}_o}{\partial \theta_o} \cdot \dot{\boldsymbol{F}}_o \right\rangle = \theta_o \frac{\partial \overline{\boldsymbol{P}}}{\partial \theta_o} \cdot \dot{\overline{\boldsymbol{F}}} - \mathrm{Div}_{\boldsymbol{X}}[\overline{\boldsymbol{Q}}] + \bar{r}. \tag{4.18}$$

In order to verify that this expression is equivalent to the macroscopic counterpart (4.14) of (2.2), the left-hand side terms may be combined as follows. Concentrating on the second term, it is noted that

$$\left\langle \frac{\partial \boldsymbol{P}_o}{\partial \boldsymbol{F}_o}\frac{\partial \boldsymbol{F}_o}{\partial \theta_o} \cdot \dot{\boldsymbol{F}}_o \right\rangle = \left\langle \frac{\partial \boldsymbol{F}_o}{\partial \theta_o} \cdot \frac{\partial \boldsymbol{P}_o}{\partial \boldsymbol{F}_o}\dot{\boldsymbol{F}}_o \right\rangle = \left\langle \frac{\partial \boldsymbol{F}_o}{\partial \theta_o} \cdot \left(\dot{\boldsymbol{P}}_o - \frac{\partial \boldsymbol{P}_o}{\partial \theta_o}\dot{\theta}_o \right) \right\rangle. \tag{4.19}$$

Here, the symmetry in $\frac{\partial \boldsymbol{P}_o}{\partial \boldsymbol{F}_o} = \frac{\partial^2 \Psi_o}{\partial \boldsymbol{F}_o \partial \boldsymbol{F}_o}$ has been made use of. Moreover, the first term in this cell average vanishes since

$$\left\langle \frac{\partial \boldsymbol{F}_o}{\partial \theta_o} \cdot \dot{\boldsymbol{P}}_o \right\rangle = \left\langle \frac{\partial \boldsymbol{F}_o}{\partial \theta_o} \right\rangle \cdot \langle \dot{\boldsymbol{P}}_o \rangle = \frac{\partial \overline{\boldsymbol{F}}}{\partial \theta_o} \cdot \dot{\overline{\boldsymbol{P}}} \tag{4.20}$$

and $\overline{\boldsymbol{F}}$ is independent of θ_o. Here, the fact that $\dot{\boldsymbol{P}}_o$ is divergence-free has been employed together with $\frac{\partial \boldsymbol{F}_o}{\partial \theta_o} = \frac{\mathrm{d}\boldsymbol{F}_o}{\mathrm{d}\theta_o}$, the former stating that $\boldsymbol{P}_o$ satisfies the cell problem (4.3) for all choices of θ_o and $\overline{\boldsymbol{F}}$. Consequently, the left-hand side of (4.18) simplifies to the expression

$$\langle c_o \rangle \, \dot{\theta}_o - \theta_o \left\langle \frac{\partial \boldsymbol{P}_o}{\partial \theta_o} \cdot \frac{\partial \boldsymbol{F}_o}{\partial \theta_o}\dot{\theta}_o \right\rangle = \left\langle c_o - \theta_o \frac{\partial \boldsymbol{P}_o}{\partial \theta_o} \cdot \frac{\partial \boldsymbol{F}_o}{\partial \theta_o} \right\rangle \cdot \dot{\theta}_o. \tag{4.21}$$

It remains to verify the interpretation

$$\bar{c} = \left\langle c_o - \theta_o \frac{\partial \boldsymbol{P}_o}{\partial \theta_o} \cdot \frac{\partial \boldsymbol{F}_o}{\partial \theta_o} \right\rangle. \tag{4.22}$$

For this purpose, macroscopic thermodynamic consistency is invoked which requires that

$$\bar{c} = -\theta_o \frac{\partial^2 \overline{\Psi}}{\partial \theta_o^2} \tag{4.23}$$

where $\overline{\Psi} := \langle \Psi_o \rangle$ is induced by (4.7) – see Temizer and Wriggers (2011) for a discussion of macroscopic thermodynamic consistency conditions. Indeed, this identification follows from

$$\begin{aligned}
\left\langle c_o - \theta_o \frac{\partial \boldsymbol{P}_o}{\partial \theta_o} \cdot \frac{\partial \boldsymbol{F}_o}{\partial \theta_o} \right\rangle &= -\theta_o \left\langle \frac{\partial^2 \Psi_o}{\partial \theta_o^2} + \frac{\partial^2 \Psi_o}{\partial \theta_o \partial \boldsymbol{F}_o} \cdot \frac{\partial \boldsymbol{F}_o}{\partial \theta_o} \right\rangle = -\theta_o \left\langle \frac{\mathrm{d}}{\mathrm{d}\theta_o} \frac{\partial \Psi_o}{\partial \theta_o} \right\rangle = -\theta_o \frac{\partial}{\partial \theta_o} \left\langle \frac{\partial \Psi_o}{\partial \theta_o} \right\rangle \\
&= -\theta_o \frac{\partial}{\partial \theta_o} \left\langle \frac{\mathrm{d}\Psi_o}{\mathrm{d}\theta_o} - \frac{\partial \Psi_o}{\partial \boldsymbol{F}_o} \cdot \frac{\partial \boldsymbol{F}_o}{\partial \theta_o} \right\rangle = -\theta_o \frac{\partial^2 \langle \Psi_o \rangle}{\partial \theta_o^2} + \theta_o \left\langle \boldsymbol{P}_o \cdot \frac{\partial \boldsymbol{F}_o}{\partial \theta_o} \right\rangle \\
&= -\theta_o \frac{\partial^2 \langle \Psi_o \rangle}{\partial \theta_o^2} + \theta_o \langle \boldsymbol{P}_o \rangle \cdot \left\langle \frac{\partial \boldsymbol{F}_o}{\partial \theta_o} \right\rangle = -\theta_o \frac{\partial^2 \langle \Psi_o \rangle}{\partial \theta_o^2} + \theta_o \overline{\boldsymbol{P}} \cdot \frac{\partial \overline{\boldsymbol{F}}}{\partial \theta_o} = -\theta_o \frac{\partial^2 \langle \Psi_o \rangle}{\partial \theta_o^2} = -\theta_o \frac{\partial^2 \overline{\Psi}}{\partial \theta_o^2} = \bar{c},
\end{aligned} \tag{4.24}$$

which completes the characterization of the macroscopic specific heat. Consequently, (4.14) can be used as the direct macroscopic counterpart of (2.2) with all macroscopic terms as cell averages except for $\bar{c}$ that is defined through (4.22).

5. Numerical investigations

In this section, numerical demonstrations of the two-phase homogenization framework are provided. Since extensive numerical results were already presented in Temizer and Wriggers (2011), the present aim is not to duplicate but rather complement the observations stated therein. Towards this purpose, the examples are grouped in two categories. First, the computational efficiency of the framework is highlighted by characterizing the deformation-induced anisotropy of the thermal response. Second, a spurious size effect that is not consistent with a separation of scales assumption, and hence with standard first-order homogenization frameworks, is discussed.

The Helmholtz free energy function in finite thermoelasticity is of the general form

$$\Psi(\theta, \boldsymbol{F}) = \frac{\theta}{\theta_{REF}} \Psi_{REF}(\boldsymbol{F}) - \frac{\theta - \theta_{REF}}{\theta_{REF}} e_{REF}(\boldsymbol{F}) + \int_{\theta_{REF}}^{\theta} \left(1 - \frac{\theta}{\theta'}\right) c(\theta', \boldsymbol{F}) \mathrm{d}\theta', \tag{5.1}$$

where $\Psi_{REF}(\boldsymbol{F})$ represents the purely mechanical response and the reference internal energy $e_{REF}(\boldsymbol{F})$ is responsible for thermal expansion. Following the entropic theory of elasticity in an isotropic setting (Chadwick & Creasy, 1984), $e_{REF}(\boldsymbol{F}) = 3\kappa\alpha\theta_{REF}\ln(\det[\boldsymbol{F}])$ is chosen where κ is the bulk modulus and α is the thermal expansion coefficient. Additionally, a volumetric-deviatoric decoupling $\Psi_{REF} = \Psi_{REF}^{vol} + \Psi_{REF}^{dev}$ is admitted for the purely mechanical response where $\Psi_{REF}^{vol} = \frac{\kappa}{4}(\det[\boldsymbol{b}] - \ln(\det[\boldsymbol{b}]) - 1)$ with $\boldsymbol{b} = \boldsymbol{F}\boldsymbol{F}^T$ and Ψ_{REF}^{dev} is modeled by a classical Ogden-type material. In order to complete the thermomechanical material model, a constant specific heat is assumed together with a Fourier-type thermal response $\boldsymbol{q} = -k\boldsymbol{g}$ on the deformed configuration where $\boldsymbol{g} = \boldsymbol{F}^{-T}\boldsymbol{G}$, $\boldsymbol{q} = \det[\boldsymbol{F}]^{-1}\boldsymbol{F}\boldsymbol{Q}$ and the conductivity k is a constant. The reader is referred to Temizer and Wriggers (2011) for the values of the material parameters employed, including the mismatch ratios between the material parameters of the individual constituents.

5.1. Deformation-induced thermal anisotropy

Within the two-phase homogenization framework, the dependence of the macroscopic heat flux $\overline{\boldsymbol{Q}}$ on the macroscopic temperature gradient $\overline{\boldsymbol{G}}$ is governed by the thermal phase only. Consequently, the characterization of thermal anisotropy can be carried out by solely varying the direction of the macroscopic temperature gradient within the thermal phase without recomputing the mechanical response, leading to significant savings in computation time in comparison with a fully-coupled thermoelastic computation. Such a characterization is summarized in Fig. 1 on a unit-cell with a single spherical inclusion at a volume fraction of 25 percent. Since an isotropic thermal conduction on the deformed configuration is assumed for the individual constituents and the macroscopic purely thermal response of such a unit cell is known to be isotropic (Torquato, 2002), the temperature gradient and heat flux vectors

$$\bar{\boldsymbol{g}} = \overline{\boldsymbol{F}}^{-T}\overline{\boldsymbol{G}}, \quad \bar{\boldsymbol{q}} = \frac{1}{\det[\overline{\boldsymbol{F}}]}\overline{\boldsymbol{F}\boldsymbol{Q}} \tag{5.2}$$

on the deformed configuration are monitored to characterize the deformation-induced thermal anisotropy. More specifically, a discrete number of $\bar{\boldsymbol{g}}$ orientations are chosen based on the 974-point angular grid of Lebedev and Laikov (1999) and a constant $\|\bar{\boldsymbol{g}}\|$ is assigned. Subsequently, for a chosen $\overline{\boldsymbol{H}} := \overline{\boldsymbol{F}} - \boldsymbol{I}$, $\overline{\boldsymbol{G}}$ is determined in order to impose periodic thermal boundary

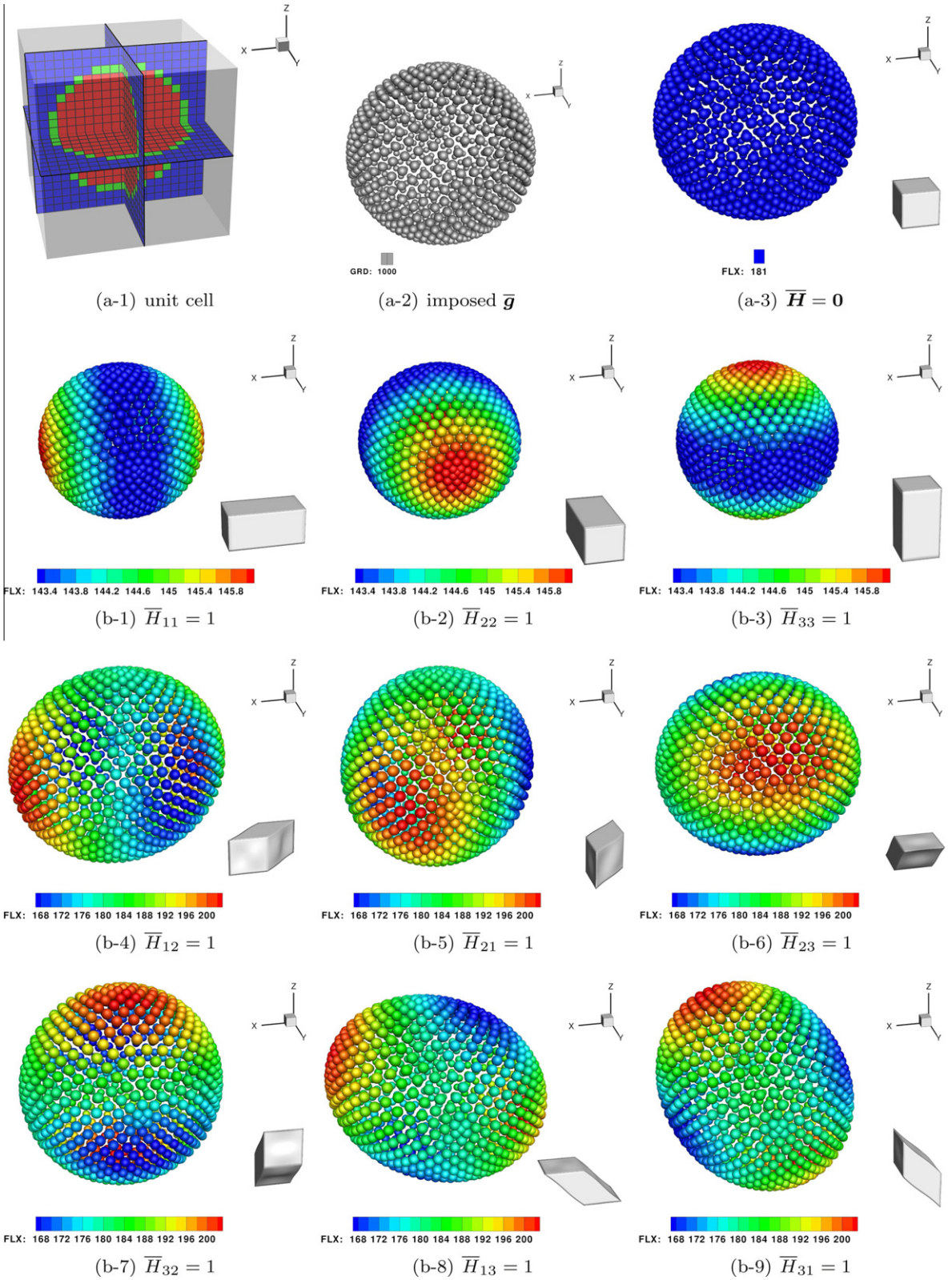

Fig. 1. The unit cell consists of a hard particle embedded in a soft matrix. 20 hexahedral elements per spatial direction are employed to discretize the unit cell. Here, the blue elements represent the matrix, the red ones correspond to the particle and green elements lie at the interface. All $\overline{\boldsymbol{H}} = \overline{\boldsymbol{F}} - \boldsymbol{I}$ components are set to zero, except for the ones which are explicitly denoted, and $\theta_o - \theta_{REF} = 10$ where $\theta_{REF} = 293.15$ K is the initially uniform temperature of the heterogeneous medium. The spatial location of a sphere represents the components of the corresponding vector. The magnitude is color-coded: $GRD = \|\overline{\boldsymbol{g}}\|$ and $FLX = \|\overline{\boldsymbol{q}}\|$. (For interpretation of the references to colour in this figure legend, the reader is referred to the web version of this article.)

conditions. The thermal phase delivers $\overline{\boldsymbol{Q}}$ as a cell average, which is then mapped to $\bar{\boldsymbol{q}}$ and plotted in Fig. 1. It is remarked that, in the present case, the periodic thermal boundary conditions can alternatively be imposed directly via $\bar{\boldsymbol{g}}$ and the deformed cell average of the microscopic flux $\boldsymbol{q}_o := \frac{1}{\det[\boldsymbol{F}_o]}\boldsymbol{F}_o\,\boldsymbol{Q}_o$ can be equivalently employed to determine $\bar{\boldsymbol{q}}$ (Temizer & Wriggers, 2011).

The perfectly spherical response in Fig. 1 for $\overline{\boldsymbol{H}} = \boldsymbol{0}$ verifies the expected macroscopically isotropic purely thermal response. Large axial deformations of the unit cell significantly alter the heat flux, although the induced anisotropy is weak compared to large shear deformations. For the latter, ellipsoidal distributions of $\bar{\boldsymbol{q}}$ clearly demonstrate deformation-induced thermal anisotropy.

5.2. Spurious size effects

The two-phase homogenization framework explicitly enforces the separation of scales assumption so that the absolute dimensions of the unit cell do not affect the homogenized response $\{\overline{\boldsymbol{P}}, \overline{\boldsymbol{Q}}\}$ for given $\{\theta_o, \overline{\boldsymbol{G}}, \overline{\boldsymbol{F}}\}$. An alternative *microscopically coupled* homogenization framework may be constructed where $\overline{\boldsymbol{G}}$ and $\overline{\boldsymbol{F}}$ are simultaneously projected onto the unit cell in the usual manner. However, the mechanical response is now influenced by the temperature distribution that is induced by $\overline{\boldsymbol{G}}$ and therefore a method of projecting θ_o onto the unit cell is additionally required. Presently, the temperature at a single corner point of the unit cell is enforced to θ_o although other approaches are possible and will display qualitatively similar problems which are to be shortly demonstrated. The microscopically coupled problem is subsequently solved through full linearization within a monolithic scheme. It is highlighted again that the macroscopic problem remains thermomechanically coupled in all cases.

Fig. 2 summarizes the macroscopic stress and heat flux responses of a unit cell with varying edge length l_{micro}, the two-phase framework results displaying no sensitivity. On the other hand, within the coupled framework the stress is influenced by the increasing temperature across the unit cell such that large sample sizes lead to larger deviations from the two-phase results. Moreover, simply by changing the direction of the macroscopic temperature gradient the stress can be influenced within the coupled framework. However, such a dependence is not consistent with the classical thermomechanical material models where the independence of the stress from the temperature gradient is typically postulated. Consequently, *these size effects are strictly spurious within a separation of scales assumption*. Indeed, as $l_{micro} \to 0$ the responses from the two alternative approaches match. The macroscopic heat flux also displays size effects. However, in this example the microscopic thermal response is postulated to be independent of the temperature and hence the size effect is only governed by the changes in the microstructural geometry due to thermal expansion. Since these changes are small within confined geometries, as in a unit cell, the measured influence of l_{micro} on the thermal response is small compared to that on the mechanical response but nevertheless significant. In particular, since $\overline{\boldsymbol{F}} = \boldsymbol{I}$ in this case, $\overline{\boldsymbol{Q}}$ should be isotropic in $\overline{\boldsymbol{G}}$ although the coupled framework clearly displays sensitivity to the direction of $\overline{\boldsymbol{G}}$.

As an alternative demonstration of the spurious size effect, random microstructures are taken as the basis of motivation. With such microstructures, one typically employs *non-periodic* (e.g. linear) boundary conditions (BCs) (Temizer & Wriggers, 2011) and it is necessary to choose a sufficiently large sample size in order to ensure that it qualifies as a *representative volume element* (RVE). Presently, the anticipated shortcomings of the microscopically coupled framework can be demonstrated by periodic microstructures. Two-dimensional microstructures are employed to reduce the computational cost and sample enlargement is carried out by varying the number of unit cells per spatial direction of a test sample (Fig. 3). As the sample is enlarged, periodic BCs within the two-phase framework display an invariant stress as well as flux response and hence are taken as the reference cases. The responses of the two-phase framework using non-periodic BCs are observed to monoton-

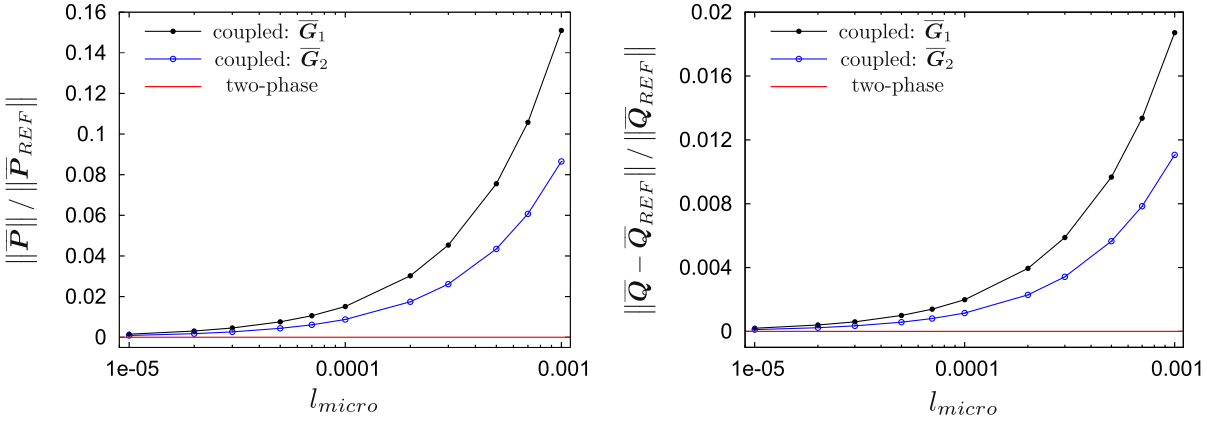

Fig. 2. The microscopically coupled framework is compared with the two-phase framework. Here, $\overline{\boldsymbol{H}} = \boldsymbol{0}$, $\theta_o - \theta_{REF} = 0$ (see Fig. 1) and all components of $\overline{\boldsymbol{G}}_1$ are set to 10^4. $\overline{\boldsymbol{G}}_2$ has the same magnitude with $\overline{\boldsymbol{G}}_1$ but is oriented in the vertical direction. The reference stress $\overline{\boldsymbol{P}}_{REF}$ is computed with the two-phase framework by assigning 0.1 to all components of $\overline{\boldsymbol{H}}$ and the reference flux $\overline{\boldsymbol{Q}}_{REF}$ by using $\overline{\boldsymbol{G}}_1$.

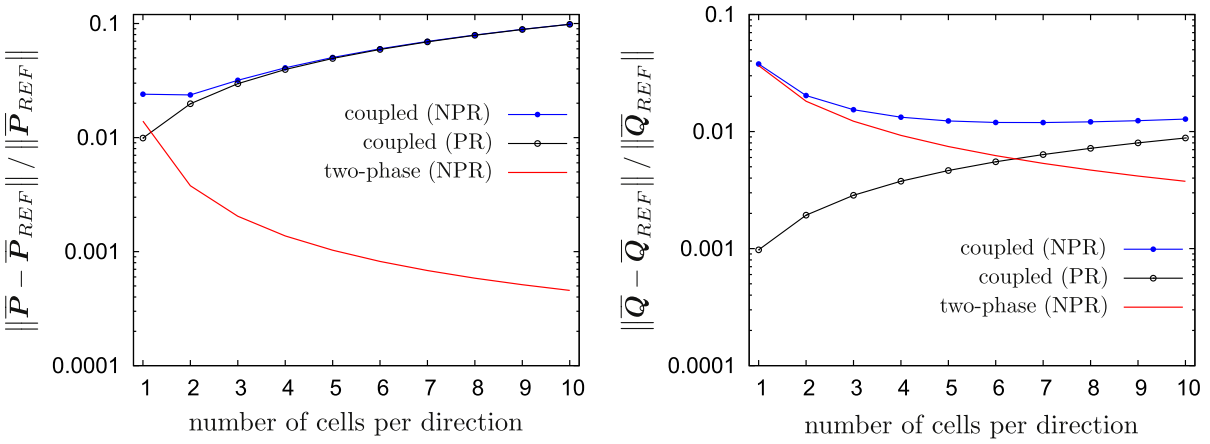

Fig. 3. The microscopically coupled framework is compared with the two-phase framework for periodic (PR) and non-periodic (NPR) boundary conditions. Here, all components of $\overline{\boldsymbol{H}}$ are set to 1, $\theta_o - \theta_{REF} = 0$ (see Fig. 1) and all components of $\overline{\boldsymbol{G}}$ are set to 10^4. The reference stress $\overline{\boldsymbol{P}}_{REF}$ and heat flux $\overline{\boldsymbol{Q}}_{REF}$ correspond to the two-phase framework with periodic boundary conditions. The absolute unit cell size is such that the radius of a particle is 10^{-4} units at a volume fraction of 25%.

ically approach the reference results which is a well-known fact and has also been demonstrated in Temizer and Wriggers (2011). Within the coupled framework, however, periodic BCs deliver results which are not constant and they monotonically diverge from the reference results. A similar response is observed under non-periodic BCs within the coupled framework and is more clearly demonstrated by monitoring the heat flux. As the sample is enlarged, the results first converge towards the response obtained under periodic BCs. With a sufficiently large sample size, the boundary condition effects are alleviated although now size effects dominate. Consequently, under sample enlargement, the response curves under periodic and non-periodic BCs converge towards each other while diverging from the results of the two-phase framework.

It is noted that the size effect in a microscopically coupled framework has two implications. First, it is necessary to vary the size of the unit cell in the range of macroscopic control parameters $\{\theta_o, \overline{\boldsymbol{G}}, \overline{\boldsymbol{F}}\}$ in order to ensure that the absolute size does not significantly influence the macroscopic response. Second, with random microstructures, the sample enlargement procedure for the determination of an RVE must be carefully monitored to avoid any spurious effect. Clearly, neither procedure is straightforward or computationally favorable, which further highlights the computational efficiency and the theoretical robustness of the two-phase homogenization framework.

6. Conclusion

An asymptotic expansion (AE) basis was provided for the first-order computational homogenization framework recently proposed in Temizer and Wriggers (2011) for finite thermoelasticity. Within an AE treatment, the separation of scales assumption is naturally enforced, yielding results that are in agreement with those obtained in Temizer and Wriggers (2011) through the monitoring of thermodynamic consistency across the scales. In particular, the AE treatment also delivered a two-phase homogenization problem posed on the unit cell of periodicity where a purely mechanical cell problem is followed by a purely thermal one. The two problems are uncoupled in the sense that only the macroscopic temperature enters the mechanical problem, and not the local temperature that is induced within the thermal one, while the thermal problem is solved at the (fixed) deformed configuration obtained from the mechanical one. The result is a computationally efficient framework on the microscale. However, this uncoupling is not a numerical one and, indeed, the coupling among the thermal and mechanical fields is preserved within the obtained macroscopic balance laws. An alternative microscopically coupled homogenization framework was additionally investigated and was shown to display spurious size effects that are not consistent with a separation of scales assumption. The agreement with the results of Temizer and Wriggers (2011) is encouraging since purely thermodynamical arguments based on explicit finite thermoelasticity formulations were pursued therein. In the context of finite deformation thermomechanical problems with inelasticity, such explicit formulations are not available and therefore it may be more advantageous to pursue an AE approach instead.

References

Aboudi, J. (2002). Micromechanical analysis of the fully coupled finite thermoelastic response of rubber-like matrix composites. *International Journal of Solids and Structures, 39*, 2587–2612.

Alzina, A., Toussaint, E., & Béakou, A. (2007). Multiscale modeling of the thermoelastic behavior of braided fabric composites for cryogenic structures. *International Journal of Solids and Structures, 44*, 6842–6858.

Chadwick, P., & Creasy, C. F. M. (1984). Modified entropic elasticity of rubberlike materials. *Journal of the Mechanics and Physics of Solids, 32*(5), 337–357.

Fish, J., & Fan, R. (2008). Mathematical homogenization of nonperiodic heterogeneous media subjected to large deformation transient loading. *International Journal of Numerical Methods in Engineering, 76*, 1044–1064.
Forest, S., Pradel, F., & Sab, K. (2001). Asymptotic analysis of heterogeneous Cosserat media. *International Journal of Solids and Structures, 38*, 4585–4608.
Francfort, G. A. (1983). Homogenization and linear thermoelasticity. *SIAM Journal on Mathematical Analysis, 14*(4), 696–798.
Francfort, G. A. (1986). Homogenization and mechanical dissipation in thermoviscoelasticity. *Archive for Rational Mechanics and Analysis, 96*, 265–293.
Khisaeva, Z. F., & Ostoja-Starzewski, M. (2007). Scale effects in infinitesimal and finite thermoelasticity of random composites. *Journal of Thermal Stresses, 30*(6), 587–603.
Kouznetsova, V. G., Geers, M. G. D., & Brekelmans, W. A. M. (2004). Multi-scale second-order computational homogenization of multi-phase materials: a nested finite element solution strategy. *Computer Methods in Applied Mechanics and Engineering, 193*, 5525–5550.
Larsson, R., & Diebels, S. (2007). A second-order homogenization procedure for multi-scale analysis based on micropolar kinematics. *International Journal for Numerical Methods in Engineering, 69*, 2485–2512.
Laschet, G. (2002). Homogenization of the thermal properties of transpiration cooled multi-layer plates. *Computer Methods in Applied Mechanics and Engineering, 191*, 4535–4554.
Lebedev, V. I., & Laikov, D. N. (1999). A quadrature formula for the sphere of the 131st algebraic order of accuracy. *Doklady Mathematics, 59*, 477–481.
Maugin, G. A. (1999). *The thermomechanics of nonlinear irreversible behaviors*. World Scientific.
Miehe, C., Schröder, J., & Schotte, J. (1999). Computational homogenization analysis in finite plasticity: Simulation of texture development in polycrystalline materials. *Computer Methods in Applied Mechanics and Engineering, 171*, 387–418.
Molinari, A., & Ortiz, M. (1987). Global viscoelastic behavior of heterogeneous thermoelastic materials. *International Journal of Solids and Structures, 23*, 1285–1300.
Özdemir, İ., Brekelmans, W. A. M., & Geers, M. G. D. (2008). FE^2 computational homogenization for the thermo-mechanical analysis of heterogeneous solids. *Computer Methods in Applied Mechanics and Engineering, 198*, 602–613.
Pavliotis, G. A., & Stuart, A. M. (2008). *Multiscale methods: Averaging and homogenization*. Springer-Verlag.
Sanchez-Palencia, E. (1980). *Non-homogeneous media and vibration theory*. Springer-Verlag.
Simo, J. C. (1998). Numerical analysis and simulation of plasticity. In P. G. Ciarlet & J. L. Lions (Eds.). *Handbook of numerical analysis* (Vol. VI). Elsevier.
Takano, N., Ohnishi, Y., Zako, M., & Nishiyabu, K. (2000). The formulation of homogenization method applied to large deformation problem for composite materials. *International Journal of Solids and Structures, 37*, 6517–6535.
Temizer, İ., & Wriggers, P. (2011). Homogenization in finite thermoelasticity. *Journal of the Mechanics and Physics of Solids, 59*, 344–372.
Terada, K., Kurumatani, M., Ushida, T., & Kikuchi, N. (2010). A method of two-scale thermo-mechanical analysis for porous solids with micro-scale heat transfer. *Computational Mechanics, 46*, 269–285.
Terada, K., Saiki, I., Matsui, K., & Yamakawa, Y. (2003). Two-scale kinematics and linearization for simultaneous two-scale analysis of periodic heterogeneous solids at finite strain. *Computer Methods in Applied Mechanics and Engineering, 192*, 3531–3563.
Torquato, S. (2002). *Random heterogeneous materials: Microstructure and macroscopic properties*. Berlin, Heidelberg, New York: Springer.
Yu, Q., & Fish, J. (2002). Multiscale asymptotic homogenization for multiphysics problems with multiple spatial and temporal scales: a coupled thermo-viscoelastic example problem. *International Journal of Solids and Structures, 39*, 6429–6452.